Multi-objective optimisation and Energy Management: adapt your ship to every mission

D Mitropoulou, MSc[a*], M Kalikatzarakis, MSc[b], Dr. T van Der Klauw [c], A.J. Blokland [d], Dr. R D Geertsma, CEng, MIMarEST[d], A M Bucurenciu, MSc[a], D Dembinskas, MSc[a]

[a]*RH Marine Netherlands BV, The Netherlands;*
[b]*Research & Technology Support - Damen Schelde Naval Shipbuilding - the Netherlands*
[c]*Netherlands Organisation for Applied Scientific Research, TNO*
[d]*Netherlands Defence Academy, The Netherlands*
*Corresponding author. Email: despoina.mitropoulou@rhmarine.com

Synopsis

Adaptability, stealth, damage sustainability, extended range and reliability are key factors to every successful naval mission. The shipbuilding industry conceptualized and deployed a wide variety of power and propulsion architectures over the decades: from mechanical, to electrical and hybrid propulsion. The tendency towards increasingly complex propulsion and power generation systems calls for the development of intelligent control strategies, Energy Management Systems (EMSs), that can handle the complexity and exploit the increased degrees-of-freedom (DOFs) of hybrid systems, while conforming to all operational constraints. In current EMSs, the aim is to save fuel costs. However, the ability to adapt to a wide variety of missions in an ever changing world is important for naval vessels. Hence, this raises the question: Can further operational gains be achieved through the use of more sophisticated integrated control algorithm, with multiple optimization goals? The present work aims to address this issue, by developing such a control system for a naval platform. The proposed EMS can modulate shipboard energy production of a hybrid propulsion plant with hybrid power supply, considering the trade-off between multiple conflicting operating goals: fuel savings, maintenance costs of on-board assets, noise and infrared signature. A validated model of a *Holland* class Patrol Vessel has been utilized to test the proposed EMS. Simulation results under varying operational profiles demonstrate the applicability, validity and the advantages of the approach.

Keywords: Energy Management; Hybrid propulsion; Multi-objective optimization

1 Introduction

The Netherlands Ministry of Defence (NL MoD) has committed to reducing its dependency on fossil fuels in its Operational Energy strategy (Netherlands Ministry of Defence, 2015) and the subsequent Defence Energy and Environment Strategy, in order to reduce the impact of its operations on the environment and in order to enhance its operational flexibility. At the same time, the Royal Netherlands Navy needs her small crew naval vessels to be adaptable to the wide variety of threats in the global theatre. The ships thus need to be able to operate with minimum energy requirement, need to have the smallest possible noise and infrared signatures and a minimum maintenance load to limit the workload on the small crews.

Hybrid propulsion, consisting of a combination of direct drive diesel engines and electric motors, and hybrid power supply, being a combination of the electric motor-generators on the shaft, diesel generators and batteries can achieve significantly reduced fuel consumption and allows for flexibility in achieving reduced signatures and maintenance loads (Breijs and Amam, 2016; Geertsma et al., 2017; Kalikatzarakis et al., 2018; Sciarretta et al.,

2014; Vu et al., 2014). Such a hybrid power and propulsion plant allows for more than one way to generate, distribute and consume energy; Thus, these additional degrees of freedom need to be continuously managed to achieve the flexible optimisation goals. Each mission with its specific optimisation goals and load profile will affect these choices and thus the vessel's optimum working point.

The introduction of Integrated Mission Management Systems (IMMS) in the RNLN allows for an automatic response of the power and propulsion plant to changing mission planning(Geertsma, 2018). The lower level control systems receive their settings from the Energy Management System (EMS) which,in turn, receives its operational goals, signature restraints and system availability from the Defect Management, Signature Management and Mission Planning modules in the Integrated Mission Management System (IMMS). The EMS establishes its control settings using a multi-objective optimisation algorithm.

Current technology allows momentary automated optimisation of electric power generation in light of a single goal: fuel saving (Breijs and Amam, 2016; Geertsma et al., 2017; Kalikatzarakis et al., 2018; Sciarretta et al., 2014; Vu et al., 2014). The results of research in EMS's indicate that much more can be gained by investing in optimisation algorithms, including multiple goals. Having the first goal achieved, a further step to optimising the operation of the ship towards minimal total cost of ownership (TCO) was taken by accounting for battery lifetime in the control system, (Mitropoulou and Elling, 2018). Most of these optimisation algorithms, however, assume convex functions for the fuel consumption and battery lifetime.

This paper proposes the application of the Nelder-Mead algorithm to solve the instantaneous optimisation of a multi-criteria objective for a number of non-convex and discontinuous functions. T which are representative for the behaviour of a hybrid power and propulsion plant on noise and infrared signature, fuel consumption and maintenance cost. While the Nelder-Mead algorithm is a direct search method, convergence to the global optimum for a non-convex, discontinuous function cannot be guaranteed. However, in a case study of a naval vessel with hybrid propulsion and power generation, we demonstrate that the method applied to the energy management optimisation problem achieves flexible operation of the plant with reduced fuel consumption, improved signatures and reduced maintenance cost, depending on the relative weight assigned to the criteria.

This paper is structured as follows. First, in Section 2, the studied system is described. While the proposed EMS can be generalized to many power generation and propulsion plants, this work focuses on a single system which is used to explain the proposed EMS and to demonstrate its feasibility. Next, the considered optimization objectives and constraints are described in Section 3.1. This is followed by a discussion on how to combine multiple, conflicting objectives into a single optimisation goal. The resulting optimisation problem is solved using the solution methods described in Section 4. The validity of the proposed solution method is demonstrated in several case studies, with varying optimisation goals . Finally, conclusions and recommendations are given in Section 6.

2 System description

This work proposes a novel optimisation strategy for the energy management on board of ships with multiple propulsion and power generation options. The proposed strategy is applicable to many configurations of power generation and propulsion plants. We apply the strategy to a case study notional frigate with a specific configuration to demonstrate feasibility. The case study configuration is given as a single line diagram in Figure 1.

The configuration used to assess the energy management strategy consists of the following components:

- 2 main engines (MEs) with 9.1 MW nominal power, each connected to its own shaft and propeller.

- 4 diesel generators (DGs) with 2.45 MW rated power.

- 2 batteries with a capacity of 1 MWh and a maximum charge/discharge rate of 5C (5 MW).

- 2 electric motors for power take in (PTI) and power take off (PTO), one on each shaft, with a nominal power of 3 MW.

Figure 1 gives a single line representation of the system, which is divided into three sections: propulsion, DC distribution, AC distribution. The propulsion section (at the top) consists of the MEs, gearboxes with their clutches, electric motors and controllable pitch propellers (CPPs). The middle part contains the DC distribution, consisting of rectified DGs connected to DC switchboards that feed several rectified auxiliary loads. The efficiency of all converters is taken into account in this study. Note that the efficiency is dependent among others on the power flow direction, i.e. whether power is delivered or absorbed. The bottom part represents the low voltage AC distribution and low voltage AC loads.

The control diagram on board the vessel is illustrated in Figure 2. This work focuses on the energy management system (EMS), depicted as tertiary control loop. The primary control layers, i.e. the converters, the governors and the active voltage regulators (AVRs), and the secondary control layers, i.e. the power management system (PMS),
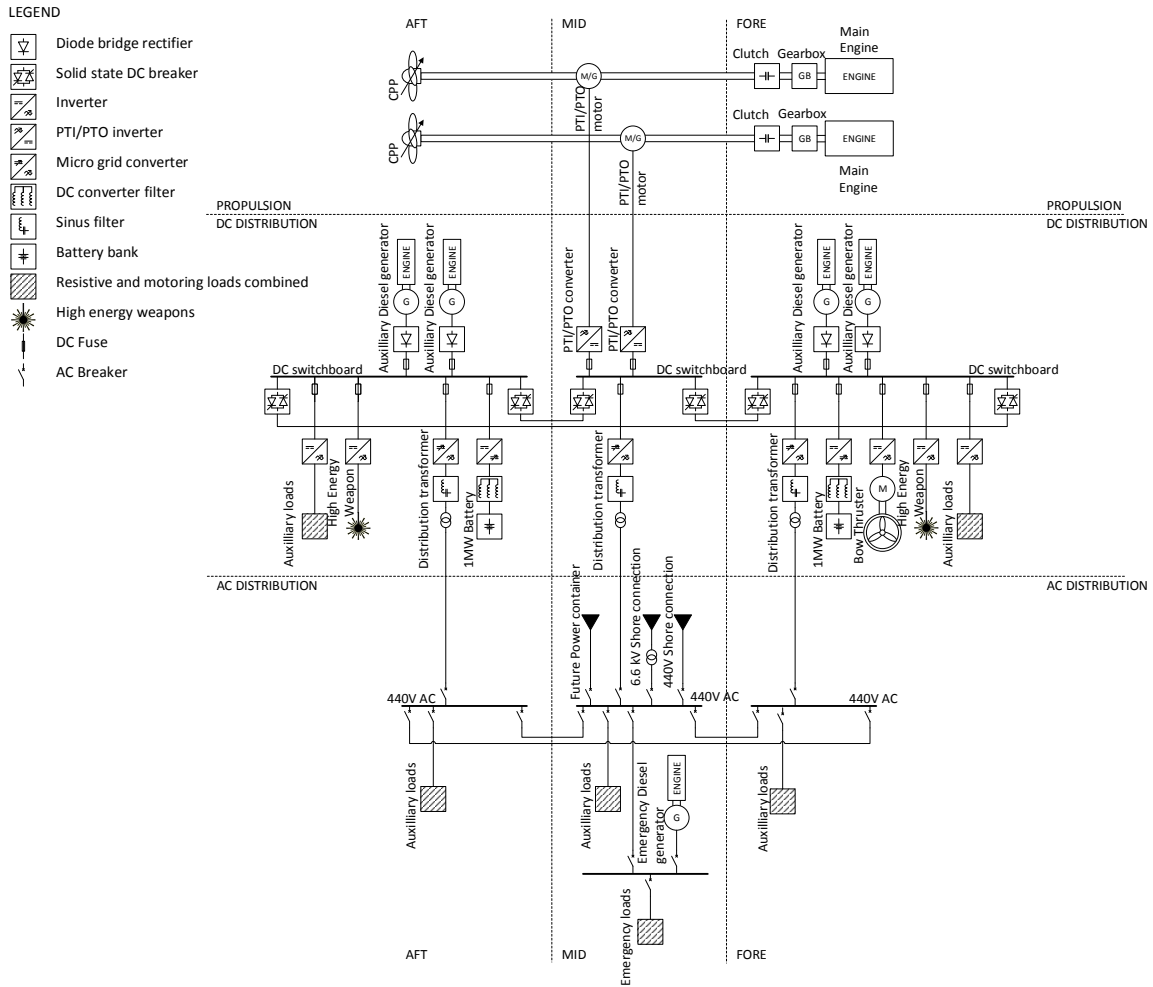
Figure 1: Single line diagram

the propulsion control system (PCS) and the battery management system system (BMS), receive information from the EMS. The main propulsion system receives inputs from the PCS, such as power and speed set points for the ME and the PTI and pitch control for the propeller. The PCS uses parallel adaptive pitch control as described in Geertsma (2019). When the motor acts as a shaft generator, i.e. PTO, it receives its power and speed set point from the PMS. The PCS gets its inputs from the lever position, autopilot data and dynamic position (DP) information. These three possible inputs result in a virtual shaft speed set point which is also provided to the EMS next to the actual shaft power feedback from the PCS.

The PMS provides power setpoints to the batteries and PTO and power and speed set points to the DGs and in turn receives feedback for the same variables. The EMS operates at one control level higher than the PMS. Thus, the EMS is responsible for allocating the power set points based on the load demand. In its turn, the PMS sends the auxiliary power as feedback to the EMS. The Integrated Mission Management System (IMMS), consisting of mission planning and signature management systems, interfaces with the EMS by defining the operational modes and converting them into weighing factors, as well as constraints.

3 Definition of the optimisation problem

In this section, the optimisation goals are described. First, we setup a system model including its operational constraints. Next, different goals for the optimisation are discussed. Finally, all goals are combined into a single objective function that can be optimized.

For the optimisation, the different, sometimes conflicting, goals need to be defined. For the present study the following are used, in no particular order: Fuel consumption, Infra red signature (IR), Life cycle cost (LCC), and Noise. The goals can be conflicting and their importance varies with the current operation mode and mission of the vessel. The importance of each goal is defined using weight factors. These factors are an input to the system from either the user or the IMMS system, as a result of different missions and operational requirements (see Section 2).
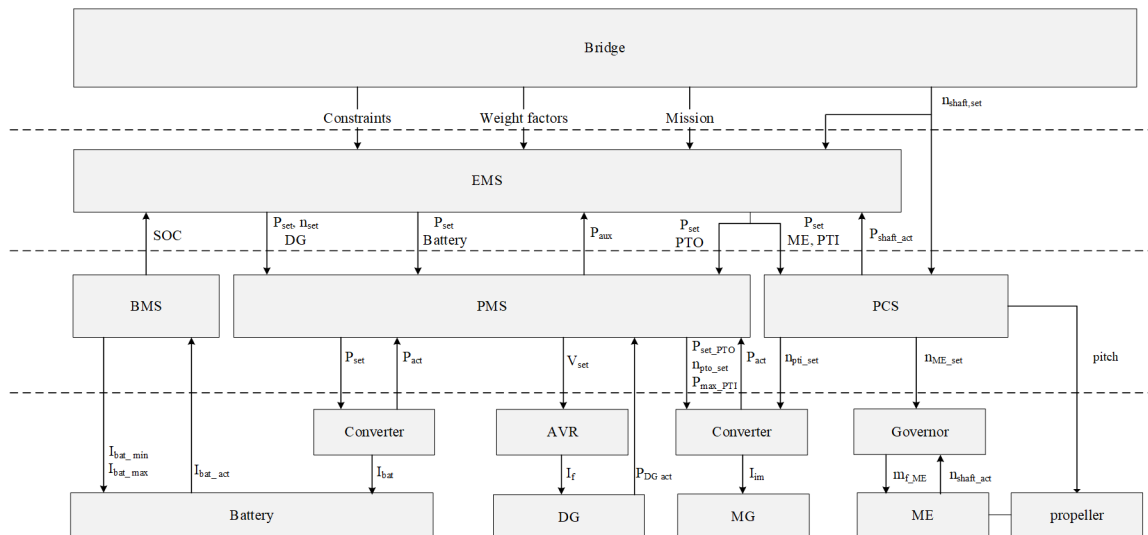
Figure 2: Control diagram

3.1 Model setup and constraints

To optimise the system described in Section 2, and particularly given in Figure 1, we describe the system behaviour with a mathematical model with control variables and inputs. As described in Figure 2, the EMS system controls the following values:

- The power output of ME i, denoted by P_{ME_i}.

- The power output and speed of DG i, denoted by P_{DG_i} and n_{DG_i} respectively.

- The power output of battery pack i, denoted by P_{bat_i}.

- The power take off or take in of EM i, denoted by P_{EM_i}.

The convention is that a negative power value means consumption. Thus, a negative value of P_{bat_i} means that the battery is charging. However, a negative value for P_{EM_i} means that the EM is generating electric power.

In order for the EMS to operate the following inputs are required:

- The propulsive power load on shaft i, denoted by P_{p_i}.

- The speed of shaft i, denoted by n_i.

- The power demand of the auxiliary loads, denoted by P_{aux}.

- The state of charge of battery i, denoted by SoC_i.

Below we first describe how we modelled each component and how we modelled the required power balance constraints to make the system run. Throughout our approach, we have used extensively polynomial regression, in which the relationship between the independent variables and the dependent variable is modelled as an n_{th} degree polynomial. To avoid overfitting, the least absolute shrinkage and selection operator (LASSO) was used, originating from (Santosa and Symes, 1986), and presented in detail in (Friedman et al., 2001). In short, this operator alters the model fitting process by selecting only a suitable subset of the provided dependent variables for use in the final model, rather than using all of them, thus in our case, reducing the order of the polynomials chosen to represent any quantity described in the following.

3.1.1 System losses and component models

The mathematical model considers the losses of the different components that can be controlled. However, grid losses are not considered because a detailed description of the entire grid aboard the vessel, since was outside the scope of the study. For the different components, losses are established as follows:

- Each ME is connected to a shaft via a gearbox, which incurs losses that are primarily determined by the power produced by the ME and the speed of the shaft.

- Each DG is used to produce electric power by driving a synchronous generator. Furthermore, the electric power output of the synchronous generator is fed to the grid through a rectifier. Losses of both the synchronous generator and rectifier are established as a function of power.

- Each battery is connected to the grid through an inverter, which incurs losses depending on its power. Furthermore, the internal efficiency of each battery is also established from the power put on or taken from the cells.

- Each EM incurs losses by converting mechanical energy to electric energy or vice versa. These losses are modelled differently for generating and motoring conditions and are based on power and speed.

For each component, we use a fourth or a second order polynomial to obtain its losses correspondingly. In other words, the losses incurred by a component *com* are given by:

$$f_{com,loss}(n, P) = \sum_{j=0}^{2} \sum_{k=0}^{2} a_{com,j,k} n^j P^k, \tag{1}$$

$$f_{com,loss}(P) = \sum_{k=0}^{2} a_{com,k} P^k. \tag{2}$$

Here, (1) is used for speed and power dependent losses of the EMs and GBs and (2) is used for power dependent losses of the battery inverter and DG rectifier.

The internal battery efficiency is given by η, which is established using:

$$\eta_{bat_i} = \frac{1}{1 + \left(\frac{P}{P_{nom}}\right)^2 R_{nom}}, \tag{3}$$

where P is the battery power put on or taken from the cell, P_{nom} is the nominal power of the cell (in our case 1MW) and R_{nom} is the nominal resistance of the cell. Note that the efficiency of the battery has a different impact if the battery pack is charged or discharged. If the pack is charged, more energy is taken from the grid than is eventually put on the cell. On the other hand, if energy is discharged, more power needs to be drawn from the cell than is put on the grid. This was modeled using:

$$P_{i,cell} = \begin{cases} \frac{P_{i,inv}}{\eta_{bat_i}} & \text{if } P_{i,inv} > 0, \\ \eta_{bat_i} P_{i,inv} & \text{if } P_{i,inv} <= 0. \end{cases} \tag{4}$$

Here, $P_{i,cell}$ is the power put on the cell of battery i and $P_{i,inv}$ is the power put on the pack after taking losses from the inverter into account. To ensure that the battery packs operate within the limits of their capacity, the state of charge of pack i is established as follows.

$$SoC_{i,new} = SoC_{i,old} + P_{i,cell} \Delta t. \tag{5}$$

Here, $SoC_{i,new}$ is the new state of charge of the pack, $SoC_{i,old}$ is the old state of charge (which is an input to the EMS) and $P_{i,cell}$ is the calculated power on the cell, taking inverter and internal losses into account. Finally, Δt is the duration the system is expected to run at the calculated set points. This value is a-priori determined by how often the EMS recalculates the optimised set points for the different control variables. The system is set to limit the newly calculated SoC between predetermined values to prevent the system from drawing too much energy from the battery and from overcharging.

3.1.2 Power balance

The primary control loop of the main engine is assumed to maintain the power balance with speed control of the governor and the used parallel adaptive pitch control strategy (Geertsma, 2019). This means that the total power on the shaft matches the propulsive power load and that the total electrical power generated matches the load of the auxiliary loads. Power balance on each shaft is modelled using:

$$P_{p_i} = P_{EM_i} + P_{ME_i} - P_{GB_i,loss}, \tag{6}$$

where EM_i and ME_i are the EM and ME connected to this shaft and $P_{GB_i,loss}$ are the losses incurred by the gearbox on the shaft. These losses are calculated as described above.

Similarly, by means of controlling the Automatic Voltage Regulator (AVR) the PMS maintains the electric power balance, as follows:

$$\sum_{i=1}^{4} P_{DG_i} + \sum_{i=1}^{2} P_{Bat_i} + \sum_{i=1}^{2} P_{EM_i,elec} = P_{aux}. \tag{7}$$

Here, $P_{EM_i,elec}$ is the electric power consumed or produced by the EM, which depends on the mechanical power take off or take in of the EM, given by P_{EM_i}, and the losses incurred by the EM (see above).

These power balances determine the main engine power from the total propulsive power load in the shafts and the electric motor/generator power setpoint and the diesel generator power from the power demand of the auxiliary loads and the power setpoints for the battery pack and the electric motor/generator power setpoint. Thus, the energy management algorithm just has to establish the setpoints for the electric motor/generator power and the battery pack.

3.2 Fuel consumption

Within the system we take into account fuel consumed by the MEs and the DGs. On top of this, we consider virtual fuel consumption by the batteries. This is done because the described EMS optimizes the set points of the equipment for the present situation, not factoring in past or future, while the battery is inherently a device that deals with energy storage over time. This means that any energy stored in the battery must have cost some fuel to charge in the past. Furthermore, charging the battery right now will cost extra fuel, but fuel can be saved later on by discharging the battery instead of generating more power with the DGs or MEs. To account for this, we include a virtual fuel cost of using the batteries. The fuel consumption of the MEs and DGs are based on fuel maps. These fuel maps are given in Figures 3(a) and 3(b) respectively. The fuel map for the MEs is split into four regions and the map for the DGs is split into five regions. These regions are marked by black bounding boxes in both figures. These regions are linked to the sequential turbocharging of the diesel engines. Switching between regions are not taken into account within this optimization. The maps are characterized by isolines of the fuel consumption (left plots for the ME and DG) given in g per kWh. To approximate the consumption values given in the fuel maps, we used a polynomial function fit to each of the regions in each of the maps. This resulted in function $f_{fuel,com,reg}(n,P)$ for the fuel consumption of component *com* when operating in region *reg* given by:

$$f_{fuel,com,reg} = \sum_{j=0}^{J} \sum_{k=0}^{K} a_{com,reg,j,k} n^j P^k, \tag{8}$$

where $a_{com,reg,j,k}$ are the coefficients for the polynomial for component *com* operating in region *reg*. Furthermore, n is the speed of the component and P its power output. Also, J and K are the degrees of the polynomial in the speed and power respectively. Figures 3(a) and 3(b) include residuals (on the right side) for the polynomial fits used in this study. These residuals are given using isolines for the percentage difference between the found approximation and the actual value on the map. It can be seen that the approximation errors lie within a few percent for both the ME and DG fuel maps.

To incorporate battery fuel cost two equivalence factors were used. These equivalence factors are denoted by Eq_{char} and Eq_{disc}. Equivalence factor Eq_{char} gives the expected future fuel saved per unit of energy charged into the battery right now. On the other hand the equivalence factor Eq_{disc} gives an estimation of the fuel costs previously incurred to charge each unit of energy. The fuel cost of a battery is obtained by multiplying the energy charged into or discharged from the pack with the respective equivalence factor, depending on whether the battery is charging or discharging. The energy taken from the battery or put into the battery can be calculated using (5). The used model gives rise to a battery efficiency and resulting equivalent fuel consumption plotted in Figures 4(a) and 4(b), where we used $Eq_{char} = Eq_{disc} = 0.055$. The choice of the equivalence factor for the battery cost function is based on the optimal operating point of the DGs. To calculate the overall fuel consumption of the system, we sum the fuel consumption of the individual components.

3.3 Noise

The noise outputs of the MEs and DGs were modelled for the noise optimisation goal. As no maps of engine noise relative to speed and power were available, we used assumed maps generated on basis of expert input, given in Figure 5(a) and 5(b) for the ME and DG noise respectively. The underlying assumption is that the MEs contain resonance frequencies an thus produce the highest noise levels at 500 and 900 rpm at 95 dB. The noise production at the lowest and highest speed (400 and 1000 rpm) are lowest, at about 20 dB lower. Furthermore, there is another dip in noise output at 750 rpm, with a reduction of about 10 dB compared to the peak. These values are then further scaled based on power output, meaning more power relates to higher noise output. The same assumptions were used for the DGs, with the values scaled for the different speed envelopes of the DGs. As with the fuel
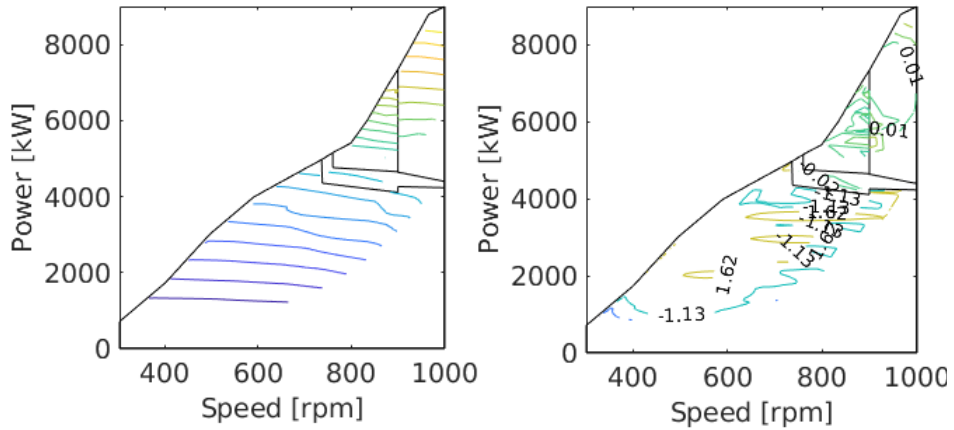
(a) ME map (left) and residuals (right).
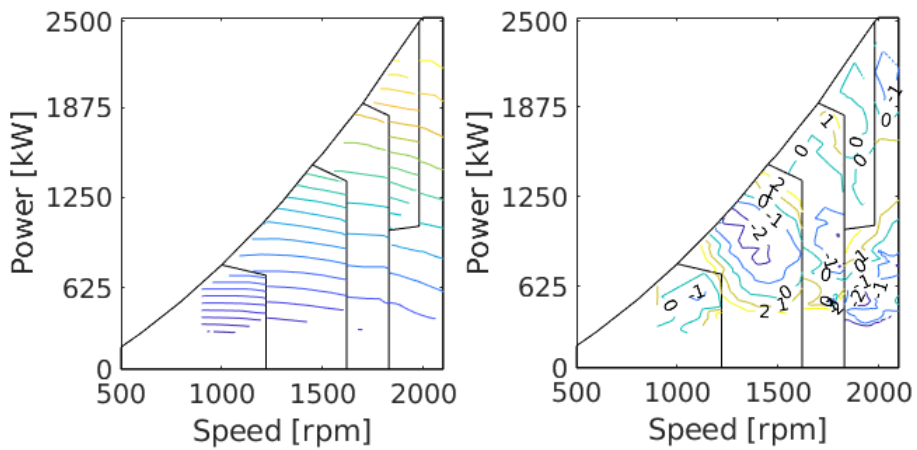
(b) Aux. DG map (left) and residuals (right).

Figure 3: Main engine (left) and Auxiliary DG (right) fuel maps (in g/s) and approximation errors (in %). Both maps are plotted using isolines to indicate the various levels of the fuel consumption or approximation errors across the envelopes of the engines. The envelopes are depicted using the solid black lines, which are also used to mark different regions in the map.

(a) Efficiency.

(b) Equivalent fuel consumption.
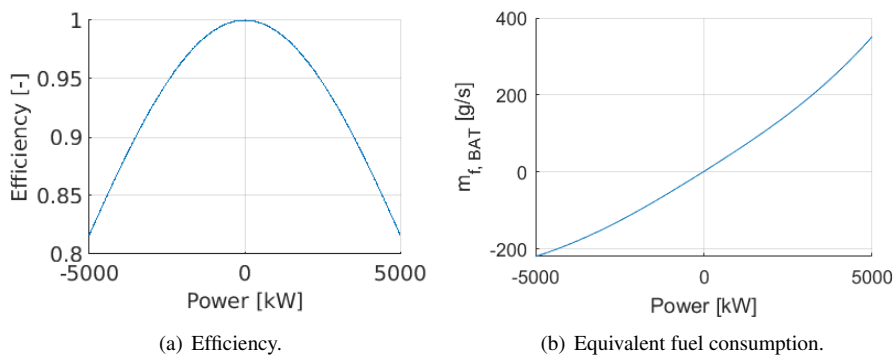
Figure 4: Battery efficiency and equivalent fuel consumption.

consumption, we approximated the produced noise by component *com* using a polynomial as follows:

$$f_{noise,com} = \sum_{j=0}^{J} \sum_{k=0}^{K} a_{com,j,k} n^j P^k, \tag{9}$$
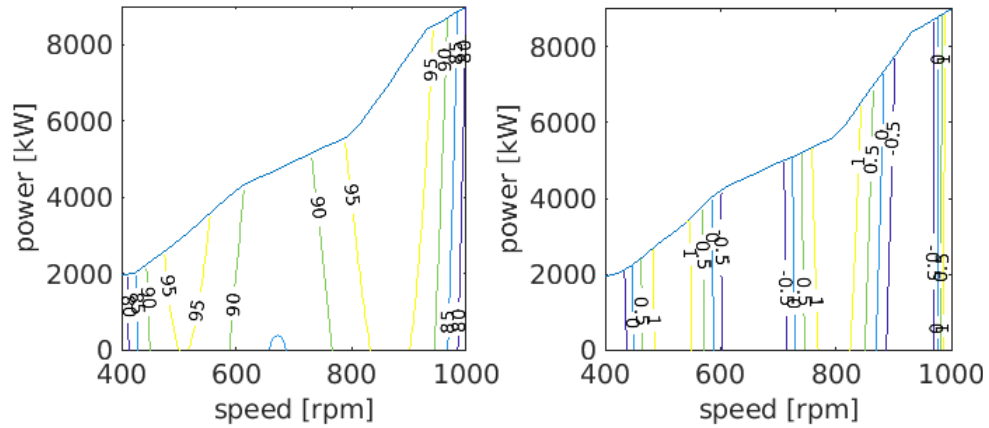
(a) ME map (left) and residuals (right).
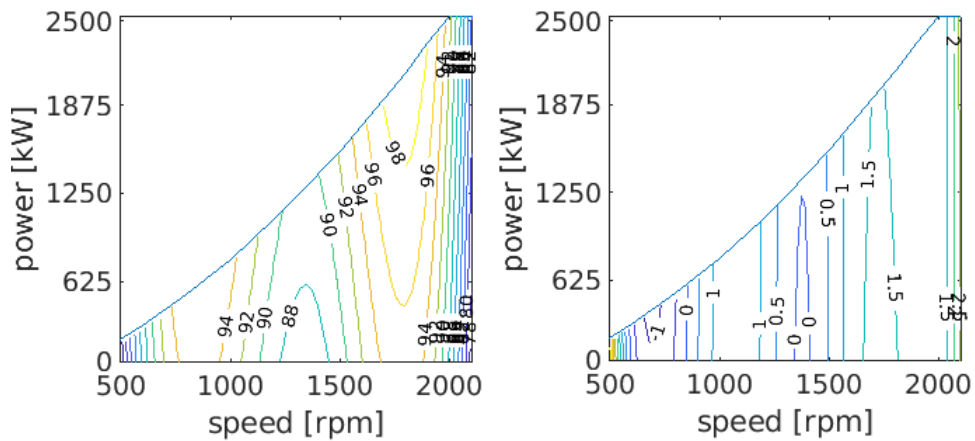
(b) DG map (left) and residuals (right).

Figure 5: Main engine (left) and Auxiliary DG (right) noise maps and approximation errors.

where n and P are the speed and power of the component and $a_{com,j,k}$ are the coefficients for the polynomial used to model the component's noise. Similar results were obtained with these approximations as for the fuel maps. The residuals for the used model and assumed maps are also given in Figures 5(a) and 5(b).

To obtain the total noise of the overall system we take the maximum of the modelled noise output of all the MEs and DGs in the system. Hence, the total noise of the system is considered to be the noise output of the loudest component.

3.4 IR

To model the IR goal, we consider only the MEs. The model map for IR output of a ME based on speed and power was generated using a high fidelity model as the product of the exhaust gas temperature times the air flow (Kalikatzarakis et al., 2018). The resulting map is given in Figure 6 and was again approximated using a polynomial function with the map separated into two regions. The resulting model map was again approximated using a polynomial function. This resulted in a modelled IR output of ME i operating in region reg given by:

$$f_{IR,i,reg} = \sum_{j=0}^{J} \sum_{k=0}^{K} a_{j,k,reg} n^j P^k. \tag{10}$$

Here n and P are the speed and power output of the ME respectively. Furthermore, $a_{j,k,reg}$ are the coefficients of the polynomial in region reg. Residuals for the used approximation are also given in Figure 6.
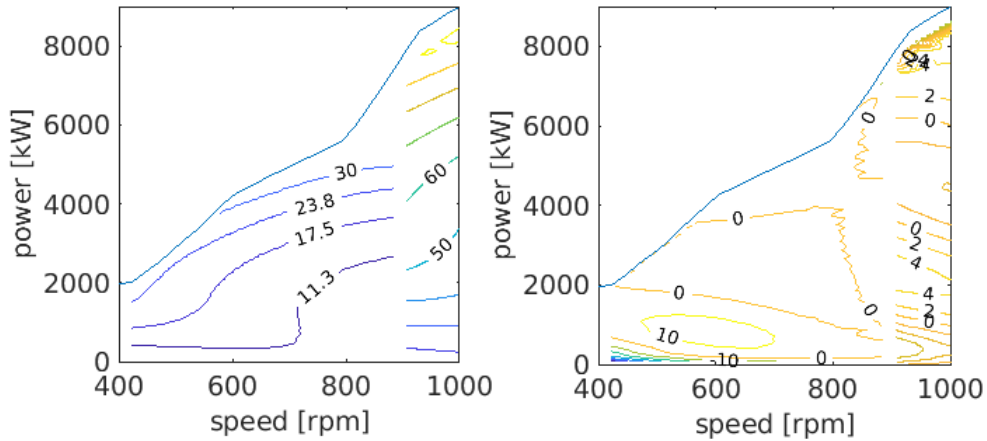
Figure 6: ME IR function (left) and residuals (right).

3.5 LCC

For the LCC goal of the optimisation only the MEs, DGs and batteries were taken into account as the LCC of these components has the greatest dependency on the working points of the main power system components. The LCC of the MEs and DGs was modelled using a fixed cost when operating, combined with a component linearly increasing with the speed of the ME and DG. Thus, the LCC of ME and DG i is given by:

$$f_{LCC,i} = a_{fixed} + a_{speed}n \text{ if } P > 0, \tag{11}$$

where the coefficients are given by a_{fixed} and a_{speed}.

The LCC of the battery was modelled in a more intricate way. This is because damage to the battery is incurred based on how much power is drained from the battery and to what depth of discharge the battery is discharged. Specifically, discharging to lower SoC values of the battery causes more degradation. Figure 7 gives a representation of the modeled battery LCC. The LCC model of the battery and the factors affecting its lifetime were based on results found in (Li et al., 2017) and (Elling, 2017). Note that we assume that no significant degradation is done to the battery during charging, as we assume the battery management system to maintain healthy heat management. The LCC of battery i is established using:

$$f_{LCC,i} = \frac{\Delta D_i a_{rpl} 3600}{\Delta t} + a_{fixed} \text{ if } P_i \neq 0. \tag{12}$$

Here ΔD_i is the degradation incurred by the discharging of the battery, a_{rpl} is a coefficient representing the replacement costs of the battery and a_{fixed} is a fixed cost for operating the battery. Furthermore, Δt is the aforementioned time at which the system is expected to operate with the given operational values.

To calculate the degradation incurred by the discharging the battery at certain SoC levels, the following model is used.

$$CTF(DoD) = \sum_{i=0}^{4} a_i DoD^{-i}, \tag{13}$$

where $CTF(DoD)$ are the current number of cycles to failure depending on the depth of discharge DoD and a_i are model coefficients. The EMS keeps track of the current DoD and calculates the new expected DoD using the currently calculated settings. It is worth to mention that the maximum allowable DoD, is a parameter than can be set, since it strongly depends on the battery technology. The degradation of the battery is calculated using:

Figure 7: Battery life-cycle cost function

$$D = \frac{1}{CTF(DoD)\varepsilon}, \tag{14}$$

where ε is a factor based on the current charge rate or current discharge rate of the battery (Li et al., 2017). The old amount of degradation incurred to the battery is tracked and the newly expected degradation is calculated based on the operating point of the battery. The resulting value of ΔD is the difference between the new degradation value and the old degradation value.

3.6 Total objective function

To be able to combine the given optimisation goals of fuel, noise, IR and LCC, as described above, the following approach is used. Note that calculated goals give values in different domains. For example, fuel consumption is established in grams per second, while noise levels are established in decibels. To be able to better compare the different objectives we first normalise them. Followed by the normalisation we multiply each objective by a weight factor. This weight factor indicates the relative priority of each of the different goals. The weight factors should each take a value within $[0,1]$ and sum to 1. The final total objective function is now obtained by summing each normalized and weighted goal. Thus, the total objective value is given by:

$$f_{obj}(x) = w_{fuel}\frac{f_{fuel}}{f_{fuel}^{norm}} + w_{noise}\frac{f_{noise}}{f_{noise}^{norm}} + w_{IR}\frac{f_{IR}}{f_{IR}^{norm}} + w_{LCC}\frac{f_{LCC}}{f_{LCC}^{norm}}. \tag{15}$$

Here f_{fuel}, f_{noise}, f_{IR} and f_{LCC} are established as described above and depend on the decided control values ($P_{ME}, P_{DG}, n_{DG}, P_{EM}$, and P_{bat}). The normalization factors f_{fuel}^{norm}, f_{noise}^{norm}, f_{IR}^{norm}, and f_{LCC}^{norm} are calculated as follows: For a given set of inputs a baseline setting is calculated. These are the values of the control inputs if the battery would not be used and the MEs generate as much of the propulsive power as possible. Furthermore, the DGs generate enough power to supply the electric loads and a minimum number of DGs is used. On top of this, the EMs are only used in motoring condition if the ME on the same shaft cannot supply the required propulsive load alone. DG power is increased accordingly, if extra power is required by any of the EMs. The values of the different optimization goals are calculated in this baseline setting. These are used as the normalising factor. This results in each different goal being calculated as a relative increase or decrease based on the baseline inputs. Hence, the objectives become comparable.

4 Solvers

To be able to optimise the power generation and propulsion plant of the vessel towards the described goals,3.6 a mathematical solver is used. There is a large amount of possible solvers available, each with their own pros and cons. In the present study, the proposed solver is the Nelder-Mead algorithm, Barton and Ivey Jr (1996). The choice for the Nelder-Mead algorithm is based on several observations. The optimisation problem at hand is non-convex and highly non-linear by nature. Furthermore, the EMS should work regardless of the specific configuration of the ship. That is, the approach should be adaptable to a system which uses a different number of components and/or components with different characteristics. Hence, a direct search method is preferred. Such an approach does not depend on specific engine characteristics. Furthermore, the Nelder-Mead algorithm has been shown to produce good results in previous work when optimising ship power generation and propulsion (van Vugt et al. (2016)). For the implementation of the algorithm some existing matlab code was used (Mathworks (2020)).

5 Optimisation evaluation

For the evaluation of the optimisation method several case studies were performed. In this section, a representative case study and the results of the optimisation algorithm per objective given a specific scenario and specific inputs are presented. For evaluating the algorithm several inputs are required, such as both port and starboard side shaft speeds. A scenario with a sailing speed of 14 knots was implemented. As a result of the sailing speed the shaft power demand for both port and starboard is 1.71 MW. The starting SoC of both battery packs was assumed to be 0.70. The auxiliary load is assumed equal to 1.65 MW. The equivalence charge factor Eq_{char} and the equivalence discharge factor $Eq_{dischar}$ that are defining the battery fuel cost are kept constant at $0,055 g/kWs$. The algorithm decides whether the batteries should be discharged, which could result in shutting down other engines, or charged, which might start one or more additional engines. The optimisation algorithm also decides which of the engines are online to minimise the objective while providing the total load demand of the system.

The significance of each optimisation goal is defined by its weight factor. The weight factors were varied, as described below, to verify results obtained when different parts of the objective are important. Note that the symbols defined here are used in Figure 10 to indicate the operating points of various equipment in the different cases.

- *Fuel* - [○] - focusing on fuel, meaning a fuel weight of 1 and other weights set to 0.

- *IR* - [+] - focusing on IR, meaning an IR weight of 1 and other weights set to 0.

- *Noise* - [∗] - focusing on noise, meaning an IR weight of 1 and other weights set to 0.

- *LCC* - [◇] - focusing on LCC, meaning an LCC weight of 1 and other weights set to 0.

- *Balanced* - [×] - focusing on a balanced objective, meaning that weight factors are set to 0.25.

- *OPEX* - [□] - focusing on OPEX, so that fuel and LCC only are taken into account. Their factors are each set to 0.5 while noise and IR get a factor of 0.

Figure 8 presents the objective values obtained through the optimisation for the different weight factors described above. Recall that the algorithm actually operates on normalised objective value, which are depicted in Figure 9. For the four individual optimisations (Fuel, IR, Noise and LCC) the resulting values are minimal amongst the different optimisation, as is to be expected. Note that in the balanced case the fuel consumption is increased significantly. This is because the algorithm can completely eliminate the IR component. This elimination (a gain of 100% reduced IR) outweighs a fuel increase of about 18%. Further contribution to the validity of this setting is that the noise and LCC values are also reduced. Finally, in the OPEX optimisation a balanced scenario between LCC and fuel optimisation is found.
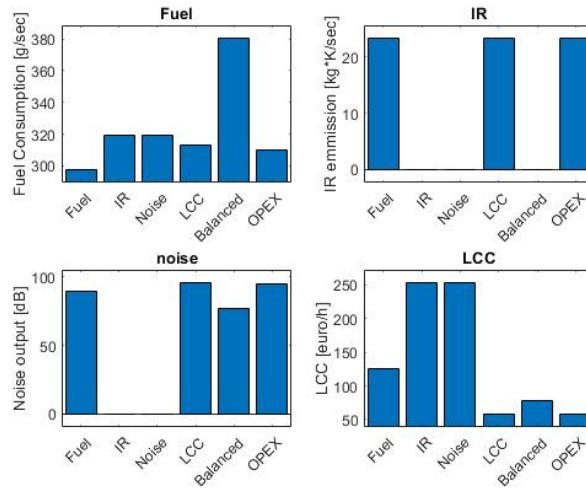
Figure 8: Objective values obtained for various settings of the weight factors before normalisation
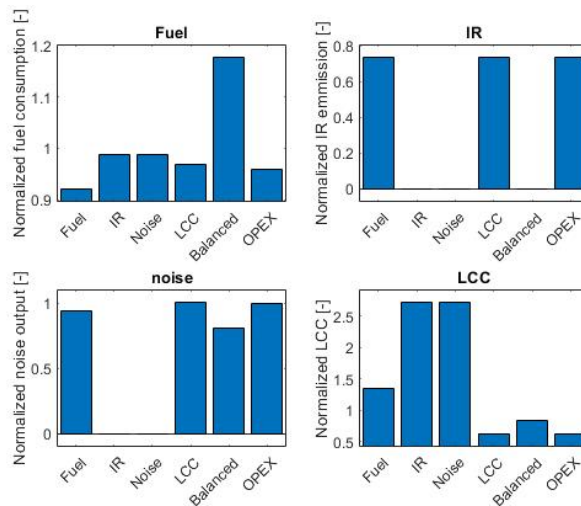
Figure 9: Objective values obtained for various settings of the weight factors after normalization

The results obtained for the different weight factors settings can be seen in Figure 10 and Table 1. The figure gives the envelopes of the MEs, DGs and EMs and their operating points per set of weight factor (for the colour coding see the list above). The table gives the numeric values of the operating points. Note, that in several cases only the starboard ME is run to provide power to both shafts. The algorithm finds this solution because the engine is much more efficient when operating at a higher power. Furthermore conversion losses in the simulated system are acceptably low to actually provide shaft power on both shafts using a single engine. If such an operating point

	Fuel	IR	Noise	LCC	Balanced	OPEX
ME port speed (rpm)	628	628	628	628	628	628
ME port power (MW)	0	0	0	0	0	0
ME starboard speed (rpm)	628	628	628	628	628	628
ME starboard power (MW)	3.7	0	0	3.7	0	3.7
DG 1 speed (rpm)	0	0	0	1833	2100	1713
DG 1 power (MW)	0	0	0	1.8	1.8	1.8
DG 2 speed (rpm)	0	0	0	0	2100	0
DG 2 power (MW)	0	0	0	0	1.8	0
DG 3 speed (rpm)	0	0	0	0	2100	0
DG 3 power (MW)	0	0	0	0	1.8	0
DG 4 speed (rpm)	0	0	0	0	0	0
DG 4 power (MW)	0	0	0	0	0	0
EM port speed (rpm)	81	81	81	81	81	81
EM port power (MW)	1.7	1.7	1.7	1.7	1.7	1.7
EM starboard speed (rpm)	81	81	81	81	81	81
EM starboard power (MW)	-1.9	1.7	1.7	-1.9	1.7	-1.9
Battery 1 power (MW)	0.9	2.7	2.7	0	0	0
Battery 2 power (MW)	0.9	2.7	2.7	0	0	0

Table 1: The operating points of the engines and the batteries found by the NM algorithm for the various optimization goals. Note that negative values for EM means the EM is used for PTO.

is infeasible or undesirable in practice due to other constraints or factors, these can be included in the model to prevent the algorithm from obtaining solutions with a single ME powering both shafts.

The algorithm decides to discharge the battery at about 1C for the case that fuel optimisation is done. This is because the equivalence factors are set such that energy in the battery is assumed to come from charging the batteries while running DGs around their optimum efficiency point. Hence, it is more efficient fuel wise to use the battery over any DGs or the second ME at low power.

For the IR and noise optimisation, the ship runs on battery power only. This is the optimum point because the battery is assumed to contribute nothing to either noise or IR. In the LCC scenario the battery is not used because it has a rather high LCC cost component. Hence the ship is running using a single ME and a single DG. Note that the choice for a single DG over turning on the port side ME is taken because the ME has a relatively high LCC component at lower load.

In the balanced scenario the ship is operated using three DGs at maximum speed and high power. This configuration completely eliminates the modelled IR output, hence a big gain is achieved there in the objective. Furthermore, the DGs are running at maximum speed because this is their operating point with minimum noise for their desired power output. The battery remains unused due to a rather large LCC increase if it would be running.

Finally, in the OPEX optimisation a balance is struck between the fuel consumption and the LCC. Because the battery has rather high LCC a single DG is used next to the starboard side ME. Note that in this case the speed of DG is further optimised (lowered) compared to the pure LCC optimisation. This is probably caused by slight differences in termination conditions of the algorithm.

6 Conclusions & Recommendations

This paper proposes a novel energy management strategy for hybrid propulsion and power generation systems for ships that can adapt to changing optimisation goals. The application of the Nelder-Mead (NM) direct search method allows optimisation of complex cost functions with non-convex and discontinuous functions. The proposed normalised relative weighing over multiple criteria and the rule-based start point of the direct search ensure the solver achieves a feasible solution while it also determines an improved and differentiated solution for different operational goals.

The results of the application on a case study naval vessel demonstrate that the performance of NM on incorporating multiple objectives is promising. It achieves improved performance on various criteria, compared to the rule-based start point of the search, which also changes when the relative weights of the criteria change. In addition, this new method can handle non-linearities and any non-convex objective functions and achieves improved solutions. The strength of the proposed approach lies in the choice of the significance per goal based on a mission.

As described the case studies for the NM method used static inputs for the equivalence factors of the batteries,

(a) Main Engines

(b) Electric Motors

(c) Diesel-generator sets
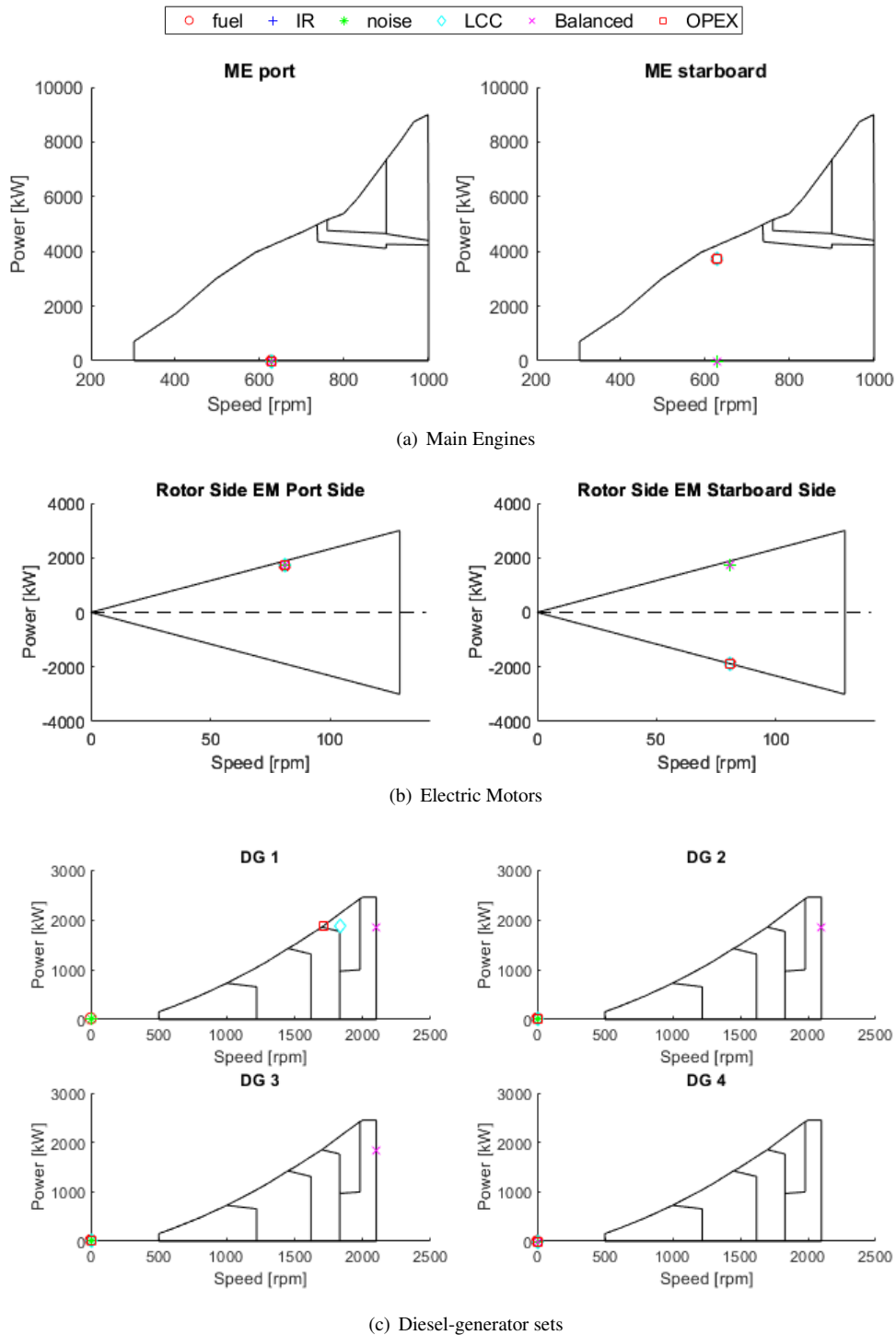
Figure 10: Operating points of the MEs, EMs and DGs for various choices of weight factors.

which results in one cost factor. Further work should focus on optimal tuning of the equivalence factors in the NM method which define the battery fuel cost continuously based on the desired behaviour of the system. Moreover, as a proof of concept of a multi-objective optimisation, extension of the NM method by incorporating other important mission objectives is recommended. Furthermore, a comparison of the NM method with other state-of-the-art linear and quadratic methods with respect to fuel consumption optimisation should be performed in order to prove that such a method does not compromise the fuel minimisation when this is the priority. Finally, a demonstration of the algorithm working real-time on a high-fidelity simulation model over a number of typical operational scenarios

should be used to demonstrate the potential improvements this autonomous control strategy can achieve over the current operator initiated operation. The realisation of such a demonstrator is due to deliver by the end of 2020.

Acknowledgement

References

Barton, R.R., Ivey Jr, J.S., 1996. Nelder-mead simplex modifications for simulation optimization. Management Science 42, 954–973.

Breijs, A., Amam, E., 2016. Energy management–adapt your engine to every mission, in: Proceedings of the 13th International Naval Engineering Conference, pp. 1–8.

Elling, L., 2017. Incorporation of battery lifetime in the energy management system of hybrid vessels.

Friedman, J., Hastie, T., Tibshirani, R., 2001. The elements of statistical learning. volume 1. Springer series in statistics New York.

Geertsma, F.D., 2018. Integration of battle damage repair management in an integrated mission management system, in: Proceedings of the 14th International Naval Engineering Conference.

Geertsma, R., 2019. Autonomous control for adaptive ships with hybrid propulsion and power generation. Ph.D. thesis. Delft University of Technology.

Geertsma, R., Negenborn, R., Visser, K., Hopman, J., 2017. Design and control of hybrid power and propulsion systems for smart ships: A review of developments. Applied Energy 194, 30–54.

Kalikatzarakis, M., Geertsma, R., Boonen, E., Visser, K., Negenborn, R., 2018. Ship energy management for hybrid propulsion and power supply with shore charging. Control Engineering Practice 76, 133–154.

Li, J., Xiong, R., Yang, Q., Liang, F., Zhang, M., Yuan, W., 2017. Design/test of a hybrid energy storage system for primary frequency control using a dynamic droop method in an isolated microgrid power system. Applied Energy 201, 257–269.

Mathworks, 2020. The mathworks. matlab fminsearch. http://www.mathworks.com/access/helpdesk/help/techdoc/index.html?/access/helpdesk/help/techdoc/ref/fminsearch.html.

Mitropoulou, D., Elling, L., 2018. New developments in energy management-battery lifetime incorporation and power consumption forecasting, in: Proceedings of the 14th International Naval Engineering Conference, pp. 1–12.

Netherlands Ministry of Defence, 2015. Operational energy strategy.

Santosa, F., Symes, W., 1986. Linear inversion of band-limited reflection seismograms. SIAM Journal on Scientific and Statistical Computing 7, 1307–1330.

Sciarretta, A., Serrao, L., Dewangan, P., Tona, P., Bergshoeff, E., Bordons, C., Charmpa, L., Elbert, P., Eriksson, L., Hofman, T., et al., 2014. A control benchmark on the energy management of a plug-in hybrid electric vehicle. Control engineering practice 29, 287–298.

Vu, T.L., Dhupia, J.S., Ayu, A.A., Kennedy, L., Adnanes, A.K., 2014. Optimal power management for electric tugboats with unknown load demand, in: 2014 American Control Conference, IEEE. pp. 1578–1583.

van Vugt, H., Sciberras, E., de Vries, L., Heslop, J., Roskilly, A.P., 2016. Ship power system modelling for the control and optimisation of multiple alternative energy sources on-board a ship, in: Proc. 15th Int. Conf. Comput. IT Appl. Martime Ind. (COMPIT), pp. 240–254.